Article

J. Biol. Regul. Homeost. Agents. 2024; 38(5): 4099–4110
https://doi.org/10.23812/j.biol.regul.homeost.agents.20243805.325

Exploration of Pathogenesis of Aortic Dissection through Whole Genome DNA Methylation

Qin Jin[1], Jie Zhang[1], Lan Shen[1], Jianqi Ni[1], Guoliang Wang[1], Liu Xu[1,*]

[1]Department of Vascular Surgery, Affiliated Hospital of Jiaxing University, 314001 Jiaxing, Zhejiang, China
*Correspondence: zhuangshenna@163.com (Liu Xu)
Published: 1 May 2024

Background: Aortic Dissection (AD) is the most common aortic emergency, and its exact etiology is still not fully understood. With advancements in molecular biology, a more profound understanding of the causes of AD will result in more significant breakthroughs in prevention and treatment. This work aimed to explore the role of genome-wide Deoxyribonucleic acid (DNA) methylation in exploring the pathogenesis and outcome mechanism of AD from the perspective of molecular biology.
Methods: Aortic tissue was collected from 8 AD patients and 8 non-AD volunteers to analyze DNA methylation characteristics in AD patients through the whole genome DNA methylation method. Based on bioinformatics, epigenetic characteristics during AD were studied. Finally, the accuracy of the chip results was verified by pyrosequencing.
Results: A total of 1563 sites were counted. Compared with the normal group, there were 942 methylation upregulated sites and 621 downregulated sites in the AD group. Differential methylation sites detected by the chip were distributed in Transmission Start Site (TSS) 1500, 5′ Untranslated Region (UTR), Genebody, 3′UTR, Cytosine, Phosphoric acid, and Guanine (CpG) island, and off-island CpG sites, mainly located in Genebody. After Gene Ontology (GO) enhancement analysis and pathway analysis of biological pathways, it was found that some methylated genes were closely related to cell differentiation, growth, maturation, aging, and death, affecting AD development.
Conclusion: Whole genome DNA methylation plays a positive role in exploring the pathogenesis and outcome mechanism of AD from molecular biology. This helps explore new diagnostic markers and intervention targets for AD and improve the clinical diagnosis and treatment of AD in the future.

Keywords: Aortic Dissection; DNA methylation; whole genome; pathogenesis

Introduction

Aortic Dissection (AD) refers to the medium-layer elastic fibers and smooth muscle degenerating and slit in the aortic wall. As a result, the blood enters the aortic membrane, causing the medium film to separate and expand along the aortic length direction to form a two-layer separation state of the aortic wall [1–5]. The onset of AD is sudden, and the condition is critical. If the dissection expands, it will cause secondary damage to multiple organs and systems, with complex clinical manifestations and various changes [6–8]. The pathogenesis of AD remains unclear. It is generally believed that the basic pathological change in AD is the degeneration of the middle layer of the aorta. Any conditions that destroy the elasticity of the middle layer or the integrity of muscle components can make the aorta susceptible to dissection [9,10]. The main risk factors include hypertension, aortic atherosclerosis (approximately 70%–90%), and aortic intimal tear [11]. With the aging population in China, AD incidence is also increasing. Foreign scholars have proven that the rate of misdiagnosis and missed diagnosis of AD patients is 39%. Despite the development of medical technology, the mortality rate of AD is still high, and postoperative complications occasionally occur [12–14]. Therefore, it is of positive significance to study the pathogenesis and outcome mechanism of the molecular biology of AD and determine its biomarkers at an early stage [15,16].

Epigenetics is a branch of genetics that studies heritable changes in gene expression without changing the nucleotide sequence of genes [17–19]. Deoxyribonucleic acid (DNA) methylation is a phenomenon in epigenetics that refers to the process of selectively adding methyl groups to cytosine to form 5-cytosine under the action of DNA methylation transferase (Dnmt) [20–22]. It is an important epigenetic marker and plays an important role in biological processes such as regulating gene expression, maintaining chromatin structure, gene imprinting, X chromosome inactivation, and embryo development [23–25]. Prasher *et al.* (2020) [26] found through experiments that epigenetics is associated with the pathogenesis of cardiovascular diseases. Normal DNA methylation is important in cell differentiation, embryo development, immunity, and defense. In contrast, abnormal DNA methylation modification is closely related to the occurrence and development of atherosclerosis, hypertension, and other diseases [27–31]. Tabaei and

Journal of
BIOLOGICAL REGULATORS
and Homeostatic Agents

Table 1. The primary materials and equipment.

Name	Manufacturer	Item number/model
Cryogenic centrifuge	Beckman (Brea, CA, USA)	allegra x-30
Low-temperature refrigerator	Thermo Scientific (Wilmington, MA, USA)	TSX70086V
Hand-held homogenizer	WIGGENS (Straubenhardt, Germany)	D-130
Ultraviolet spectrophotometer	RUNQEE Instrument Technology Co., Ltd. (Shanghai, China)	G-9
Constant temperature water bath	Zhicheng Analytical Instrument Manufacturing Co., Ltd. (Shanghai, China)	ZSXH-618
Thermal cycler	Thermo Scientific (Wilmington, MA, USA)	A24811
Oscillator	Namerui Electronic Technology Co., Ltd. (Suzhou, China)	YCL-300A
Vacuum pump	EDWARDS (Crowley, UK)	E2M1.5
Electrophoresis apparatus	Liuyi Biotechnology Co., Ltd. (Beijing, China)	DYCZ-28B
Hybrid furnace	Tianshi Scientific Instruments (Shanghai, China)	GSL-1700X-50VTB
Methylation kit	Baiaolaibo Technology Co., Ltd. (Beijing, China)	WK146
Phosphoric acid buffer salt solution	Codow (Guangzhou, China)	CD432913
Buffer ATL tissue lysis buffer	Qiagen (Dusseldorf, Germany)	19076
Protease K	Hzymes Biotechnology Co., Ltd. (Wuhan, China)	HH4500
Ribonuclease A	Sigma-Aldrich (Shanghai) Trading Co., Ltd. (Shanghai, China)	9001-99-4
99.5% ethanol solution	Baiaolaibo Technology Co., Ltd. (Beijing, China)	GL2373
Buffer AW1 and AW2 solutions	Qiagen (Dusseldorf, Germany)	1067924/1020955
Agarose powder	LONZA (Basel, Switzerland)	50150
Elution buffer	Perfemiker Reagent (Shanghai, China)	PM12158

Tabaee (2019) [32] noted that in atherosclerotic plaques, the level of DNA methylation showed a downward trend in the tissue genome, which would cause the proliferation of smooth muscle cells, thus leading to the development of atherosclerosis. However, some studies found that [33,34] abnormal DNA methylation modification may affect the expression of some candidate genes of hypertension and then affect the whole development process of the disease. Current clinical studies show that DNA methylation modification is related to cardiovascular diseases, and the overall methylation level of genomic DNA and the level of DNA methylation transferase are involved in the course and outcome of cardiovascular diseases. The role of epigenetic regulation in the phenotypic transformation of smooth muscle cells has also been observed in aortic disease [35,36]. UHRF-1 is an important regulatory protein that maintains DNA and histone methylation. It can directly restrict the expression of cell cycle suppressor gene promoters and essential cell pro-differentiation genes to promote the phenotypic transformation of smooth muscle cells during the development of aortic disease. In contrast [37], ARHGAP-18 inhibits the phenotypic transformation of smooth muscle cells and protects aortic walls. In some dedifferentiated smooth muscle cells, downregulating the expression of DNA demethylase can improve the level of DNA methylation and restrict the binding of promoters of genes related to the contractility phenotype of smooth muscle cells to RNA polymerase [38].

Therefore, AD and cardiovascular diseases are closely associated with DNA methylation. Starting from epigenetics, it is significant to study AD's pathogenesis and outcome mechanism from a molecular biology [39]. Finding the pathogenesis and early diagnosis targets of AD is crucial for reducing the prevention and diagnosis of AD, and suitable noninvasive intervention targets are of great value for the complete cure of AD. In this study, whole genome DNA methylation analysis was performed to verify the aortic tissue samples of AD patients and non-AD patients, identify the DNA methylation characteristics of AD patients, and study the epigenetic characteristics of AD patients based on bioinformatics. Finally, pyrosequencing was carried out to verify the accuracy of the chip results. The study was expected to provide a reference for the clinical diagnosis and treatment of AD by exploring the pathogenesis and outcome mechanism from molecular biology.

Materials and Methods

Research Subjects

Aortic tissue was collected from 8 AD patients who received open surgical treatment at the Affiliated Hospital of Jiaxing University and 8 non-AD patients. Meanwhile, general clinical data of all patients were collected, including name, sex, age, height, weight, smoking and alcohol history, and past medical history.

Inclusion criteria for the AD group: (1) No previous history of AD; (2) Receiving open surgery in our hospital. Exclusion criteria: AD arising from Marfan syndrome, Ehlers-Danlos syndrome, Erdheim medial necrosis, Behcet's disease, pregnancy, syphilis, endocarditis, systemic lupus erythematosus, or multiple tuberous arteritis.

Inclusion criteria for the normal group were voluntary cadavers with normal organs and no history of immune system diseases, genetic diseases, tumors, or other serious diseases. Aortic tissue sample collection was performed within 6 to 8 hours of the subject death, ensuring sample quality and integrity.

DNA was extracted from aortic tissue samples. After heavy sulfite treatment, using the human DNA methylation microarray chip (Human Cytosine, Phosphoric acid, and Guanine (CpG) Islands, 44K×1, Agilent Technologies Co., Ltd., Santa Clara, CA, USA) was used to analyze and screen it. Finally, the methylation difference sites were counted. This article involves the collection, processing, and analysis of human subjects and human tissue samples, already in accordance with the ethical principles of the Declaration of Helsinki. Ethical Approval: This article has been approved by the Ethics Committee of the Affiliated Hospital of Jiaxing University (Ref. 20210567) and strictly complies with international ethical guidelines. Subject informed consent: All human subjects who participated in the trial signed an informed consent form before participation; the purpose, sampling procedures, potential risks, and benefits of the trial were explained in detail. Privacy and confidentiality: The research team has taken measures to ensure the personal privacy of the subjects and the confidentiality of the data, and all data are processed in anonymous form.

Main Experimental Instruments, Materials, and Reagents

The primary materials and equipment information used in the experiment are shown in Table 1.

Human DNA Methylation Microarray Chip and Analysis Software

Human DNA methylation microarray chip (Agilent Technologies (China) Co., Ltd., Beijing, China) and Methylumi chip data analysis software (version: 2.4.0, https://www.bioconductor.org/help/search/index.html?search-Bar=Methylumi/) were used. Methylumi is an open-source software package jointly maintained and developed by independent researchers and the developer community, not developed by a specific company.

DNA Extraction and Concentration Determination of Aortic Tissue

After the intact aortic tissue was obtained, the normal and pathological parts were cut into a square of approximately 1.0 cm × 0.5 cm and preserved with liquid nitrogen for subsequent experimental research.

The tissue (<100 mg) was placed in a mortar, strictly following the instructions. At the same time, liquid nitrogen was added, followed by grinding to powder. Then, the power was transferred to a 2 mL centrifuge tube, and 70 μL phosphate buffer salt solution was poured in, followed by beating with a hand-held homogenizer until it was particle-free. Next, 100 μL of buffer ATL tissue lysis buffer and 20 μL of protease K were added, and the mixture was incubated at a constant temperature of 60 °C until the aortic tissue was completely lysed. Subsequently, 4 μL Ribonuclease A (RA) (100 mg/mL), 200 μL tissue lysis buffer, and 200 μL 99.5% ethanol solution were added sequentially, followed by incubation at room temperature and centrifugation. Then, 500 μL Buffer AW1 and AW2 were introduced successively, followed by centrifugation at 10,000 rpm for 2 min at high speed, and the supernatant was collected. Finally, 30 μL double steam water was added for incubation for 1 minute, followed by centrifugation at a frequency of 7000 rpm for 1 minute. After elution, the extracted tissue DNA was tested. The instrument used the ultraviolet spectrophotometer to detect the absorbance value of sample DNA at wavelengths of 260 nm and 280 nm, thus identifying sample DNA concentration and optical density values. Finally, 5 μL of the sample was added to 1% agarose gel wells, and electrophoresis at 100 V constant pressure was performed for 40 minutes.

Human DNA Methylation Microarray Chip Detection Process

Tissue DNA was treated with bisulfite. The conversion reagent and washing buffer were prepared in advance according to the kit requirements.

The experimental process was as follows.

Day 1: Each 96-well plate was labeled with barcode labels. The tissue DNA was denatured according to the requirements of the methylation kit, incubated in a 60 °C incubator for 24 hours, and then cycled using a thermal cycler. After 15 cycles, the temperature of the thermal cycler was maintained at 5 °C, and the tissue DNA was placed in it for later use.

Day 2: It should strictly follow the kit instructions. After washing and removing the conversion reagent, it was placed in the desulfonation buffer reaction stop solution for 20 minutes at constant temperature and then washed. The elution buffer was added again and centrifuged at 10,000 rpm for 10 minutes. After the gDNA was eluted, it was stored for later use (–15 °C–25 °C). The multiplication-stimulating factor (MSA4) reagent was prepared according to the alkaline denaturation-genome whole amplification extraction method. The preparation process was as follows. It should dilute 1 M sodium hydroxide to 0.1 M, mark the MSA4 well plate, add 20 μL of MA1 and sulfite-treated DNA samples, and mark the corresponding ID. Next, 4 μL of sodium hydroxide was added to each well to cover the septum of the 96-well plate to ensure correct correspondence with no splashing or contamination. Then, they were mixed for 1 minute using a shaker at 1500 rpm and centrifuged at 260 for 1 minute. After 15 minutes of incubation at room temperature, 60 μL of rpm and 70 μL of MSM were added, covered with the membrane, inverted 10 times to mix thoroughly, centrifuged at high speed for 1 minute, and then placed in a hybridization oven at 37 °C for 24 hours.

Day 3: MSA4 was centrifuged for 1 minute, and 50 μL of soluble FMS tyrosine kinase was added to cover the membrane. They were mixed well using a shaker at 1500 rpm for 1 minute and incubated in a heating block at 37 °C for 1 hour. After 100 μL PM1 was added to the MSA4

Journal of
BIOLOGICAL REGULATORS
and Homeostatic Agents

well, it was covered with a diaphragm, mixed with a shaker at 1500 rpm for 1 minute, incubated at 37 °C for 5 minutes, and centrifuged at high speed for 1 minute. After the addition of 250 μL of 100% isopropanol to the well, it was covered with a septum, turned up and down 10 times to mix well, and then placed in a 4 °C refrigerator for 30 minutes. Next, the sample was centrifuged for 20 minutes, and the supernatant was discarded. It was placed upside down on absorbent paper, and the blue precipitate was carefully removed and stored for later use (–15 °C–25 °C).

For resuspension, 40 μL of RA1 was added to the MSA4 well, sealed, and incubated in a hybridization oven at 45 °C for 1 hour, mixed well with a shaker at 1600 rpm for 1 minute, and centrifuged at high speed for 1 minute until the blue precipitate was resuspended. During hybridization, the hybridization box was opened, 400 μL of PB2 was added, and the box was immediately closed to prevent volatilization. The resuspended MSA4 was denatured at 95 °C for 20 minutes, cooled naturally, and centrifuged at high speed for 1 minute. It should take the chip out of the box and let it stand, put it into the Hybridization (Hyb) Chamber inserts, add 15 μL of DNA samples to the chip loading area in sequence, and record the corresponding ID. Then, the Hyb Chamber inserts carrying the chip were placed into the hybridization box, incubated in the hybridization oven at 48 °C for 20 hours after closing, added to 300 mL of 100% ethanol, mixed well, and cooled naturally.

Day 4: After 200 mL of PB1 was added to the washing plate, 95% formamide, 1 mM Ethylene diamine tetraacetic acid (EDTA), and 1 mL of a human DNA methylation microarray chip were added, and the temperature was adjusted to approximately 45 °C. The chip was removed from the hybridization box, placed on the washing rack, lifted, and pulled up and down. It should be noted that it had to leave the liquid surface each time for 1 minute. It was placed in the second wash dish and repeated the above operations. The chip was placed in the black frame to ensure it was submerged by PB1 and then placed in a clean glass back plate. After adding 150 μL RA1 to the glass back plate in sequence, it was incubated for 30 seconds, which was repeated 5 times: 400 μL XC1, incubation for 10 minutes; 400 μL XC2, incubation for 10 minutes; and 200 μL TEM, incubation for 15 minutes. Then, 400 μL 95% formazan Amide/1 mM EDTA was added for 6 minutes. The above operation should be repeated once. Next, it can turn on iScan, add 200 μL of SEM to the slope of the glass back plate in sequence, and let it stand for 10 minutes, which should be repeated 3 times. Then, 400 μL XC3 was allowed to stand for 5 minutes 4 times, and 200 μL ATM was allowed to stand for 10 minutes once.

Then, 300 mL of PB1 was added to the first wash pan, and the staining rack was placed. The chip was removed and placed into the staining rack, lifted up and down 10 times, and soaked for 5 minutes. Then, 300 mL of XC4 was added to the second washing plate, and the chip was lifted, pulled up and down 10 times, and soaked for 5 minutes. The chip was removed and placed on a tube rack with the front side up, dried in a vacuum pump for 1 hour, wiped to ensure it was flat, and placed in a vacuum pump at room temperature for chip scanning.

Chip Results Verification by Pyrosequencing

Single aortic tissue samples underwent polymerase chain reaction (PCR) product purification and were annealed with primers in a vacuum workstation environment. Then, they are imported into the PSQ96 MA technology platform (972804, Qiagen, Uppsala, Sweden). Pure water (600 μL) was added to dissolve the substrate fully. Next, the Q96 card clip is aligned, and the corresponding reagent is added to the corresponding well. Subsequently, the card clip was placed in a PyroMark Q48 sequencer to adjust to the appropriate position, and sequencing was carried out. The above operations were repeated 3 times to complete the sequencing.

Methods for Statistics

The experimental data were processed using SPSS 20.0 statistical software (20.0, IBM Corporation, Armonk, NY, USA), and the mean values of continuous variables were expressed as ± standard deviation. Independent sample *t*-tests were employed for comparisons between two groups, while the *chi*-square test was utilized for categorical variables (such as "smoking/alcohol history" and "hypertension/diabetes"). A significance level of $p < 0.05$ was considered statistically significant. Processed chips were placed in a scanner, which acquired fluorescence signals and generated raw data. The location of the scan results was recorded, and the obtained data were directly imported into Genome Studio software for analysis. The Illumina official base calling algorithm was used to obtain the raw signal intensity values for each locus. Genome Studio software, developed by Illumina Inc. (v1, San Diego, CA, USA), was employed for this purpose. Subsequently, bias correction and normalization were performed due to different fluorescence and probe types. After site filtering, the normalized methylation levels of high-quality CpG sites, represented by β values, were obtained for quality control. Pearson correlation coefficients (PCC) between samples were calculated to assess the reproducibility of chip signal quality, where a β value of 0 indicated unmethylation at the locus, and a β value of 1 indicated complete methylation. The quality-controlled data were subjected to differential methylation analysis using the IMA R package (3.1.2, https://ima.r-forge.r-project.org/), employing the empirical Bayes statistical method from Limma. Identification of differentially methylated genes occurred when the obtained results showed a difference score <-13 or >13 and DeltaBeta >0.17 or <-0.17 (DeltaBeta represents the difference in the average β value for each methylation site between the control and experimental groups). DeltaBeta analy-

Table 2. Basic information of patients providing aortic tissue samples.

Basic data	Aortic Dissection group (n = 8)	Normal group (n = 8)	t/χ^2 value	p-value
Age (years old)	48.4 ± 5.2	45.8 ± 5.4	1.001	0.334
Gender (male/female)	5/3	4/4	0.254	0.614
Height (cm)	165.41 ± 4.82	166.18 ± 4.37	–0.339	0.739
Body weight (kg)	64.67 ± 6.82	65.29 ± 5.98	–0.193	0.850
History of alcohol and tobacco	3	3	0.000	1.000
History of hypertension	2	1	0.410	0.522
History of diabetes	2	2	0.000	1.000

sis involved enrichment statistics for Gene Ontology (GO) terms associated with genes related to the corresponding genomic loci. This analysis quantified the number of differentially expressed genes within GO terms and determined the significance of the enrichment through statistical tests. Pathway analysis of genes corresponding to differentially methylated sites was performed using the Harmonomeme database (https://maayanlab.cloud/harmonizome/) to assess their importance in pathways.

Results

Basic Information of Patients Providing Aortic Tissue Samples

Aortic tissue was collected from 8 AD (Aortic Dissection) patients who underwent open surgery and 8 normal volunteers who had never suffered from AD. The specific clinical information of the subjects is shown in Table 2. There was no significant difference in sex, age, or other relevant information between the two groups ($p > 0.05$), which was comparable and had a negligible impact on the results of this experiment.

Sample Quality Test Results

The test results of DNA extraction are shown in Table 3. The A_{260}/A_{280} ratio of aorta tissue samples extracted from the AD and normal groups was greater than 1.7 and less than 1.9, respectively. The samples' concentration and purity met the requirements of DNA methylation chip detection, so the detection was qualified. Fig. 1 shows that multiple uniform, clear, and bright DNA bands appeared in the electrophoresis process, indicating successful DNA extraction.

Conversion Effect Evaluation

Before testing the chip, DNA was extracted, sulfites were converted to ensure that the experimental results were concrete and convincing, and strict quality control was carried out. Four quality control probes were used to detect unconverted methylation and converted unmethylated templates at a site. If the sulfite conversion is successful, the probe is labeled with red fluorescence. If the red channel generates a high signal value and the green channel a low signal value, the conversion effect is good. The results are shown in Fig. 2. The four quality control probes generated high signal values in the red channel and low signal values in the green channel, indicating a good conversion effect and a successful experiment.

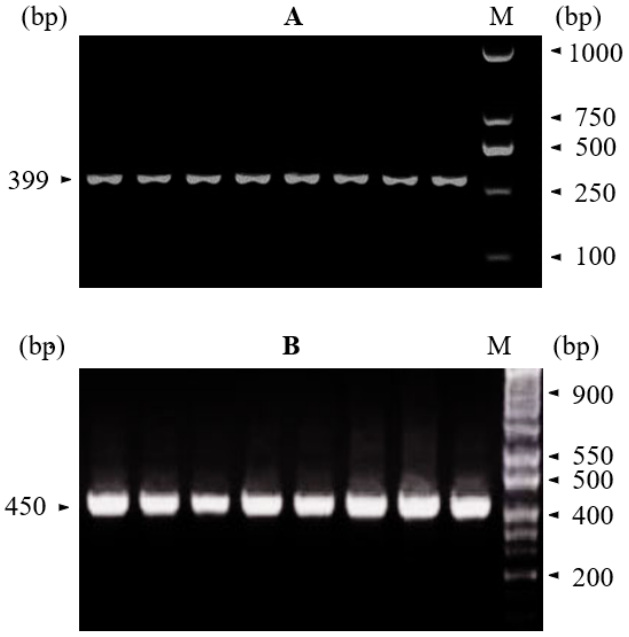

Fig. 1. Electrophoresis results. (A) shows the Aortic Dissection (AD) group, and (B) shows the normal group. After agarose gel electrophoresis, 399 bp size amplification products were visible in the AD group, and 450 bp size amplification products were visible in the normal group; M is DNA Marker.

Scatter Plot of Methylation Microarray Scan Data

Fig. 3 shows the distribution trends of AD and normal groups using the mean beta values of the two groups. Each point was a chip detection point, the X-axis was the normalized signal value of the point in the chip, and the Y-axis was the normalized signal value of the point in the control chip. It can be observed from the Fig. 3 that with the increase of normalized signal value, the corresponding normalized signal value increases, and the trend is linearly distributed.

Journal of
BIOLOGICAL REGULATORS
and Homeostatic Agents

Table 3. Sample quality test results.

Number	Original sample volume (μL)	ng/μL	A_{260}/A_{280}	Current sample volume (μL)	Rating
AD group					
76867	35	137.4	1.71	30	Qualified
75657	35	119.5	1.83	30	Qualified
35322	35	83.8	1.75	30	Qualified
43455	35	124.1	1.74	30	Qualified
21323	35	69.3	1.88	30	Qualified
35436	35	78.2	1.70	30	Qualified
23125	35	108.5	1.76	30	Qualified
76876	35	57.7	1.82	30	Qualified
Normal group					
54364	35	67.6	1.86	30	Qualified
45365	35	89.4	1.85	30	Qualified
34546	35	67.6	1.84	30	Qualified
34907	35	82.1	1.74	30	Qualified
23435	35	75.2	1.67	30	Qualified
45667	35	74.7	1.69	30	Qualified
74478	35	96.3	1.83	30	Qualified
35446	35	102.6	1.78	30	Qualified

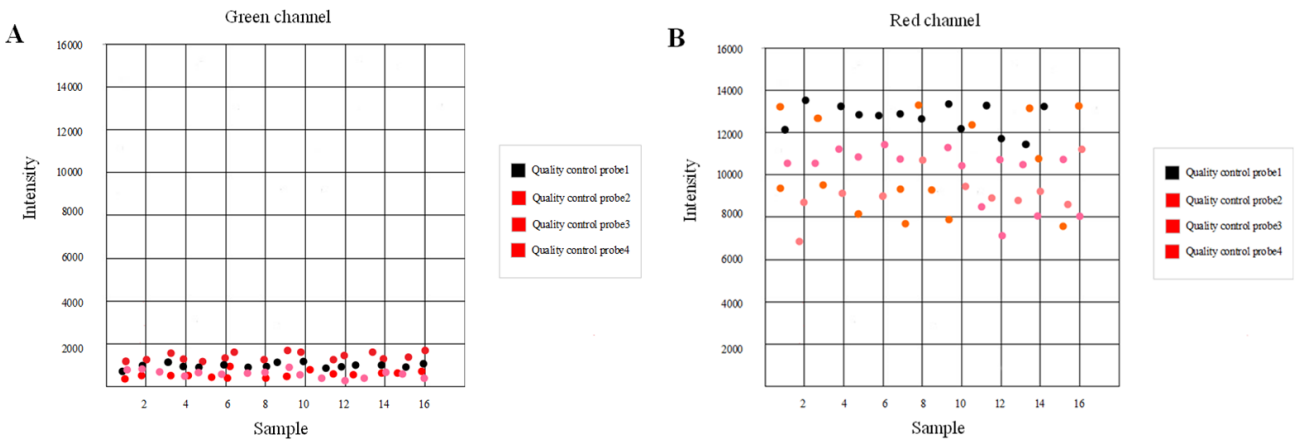

Fig. 2. Probe conversion results. (A) is the green channel, and (B) is the red channel.

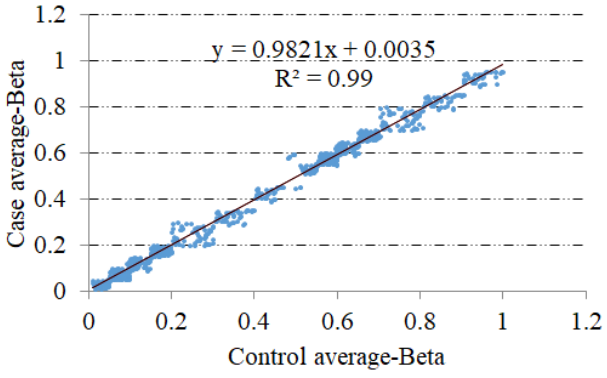

Fig. 3. A scatter plot using the average of the beta values.

DNA Differential Methylation Site Screening

Differential methylation sites refer to the difference score <–13 or >13 and DeltaBeta >0.17 or <–0.17 in the aortic tissue samples of the AD and normal groups. In this experiment, a total of 1563 sites were counted. Compared with the normal group, there were 942 methylation upregulated sites and 621 downregulated sites in the AD group. Fig. 4 shows the distribution of differential methylation sites detected by the chip in each region of the gene. Differential methylation sites were mainly located in the Genebody. The top 10 upregulated and downregulated methylation sites are shown in Tables 4,5.

GO Analysis

GO analysis was used to analyze the genes corresponding to differential methylation sites, and the number of differential genes contained in them was counted. When

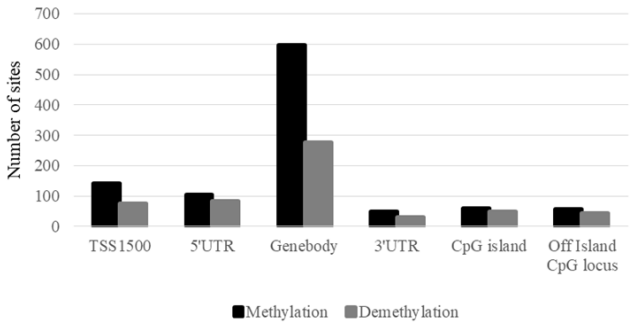

Fig. 4. Distribution of differential methylation sites in various regions of genes. UTR, Untranslated Region; CpG, Guanine; TSS, Transmission Start Site.

Table 4. Top 10 upregulated sites of differential methylation sites.

Site	Code	Location	Difference value
PQLC1	cg13244245	18	38.96528
MYT1L	cg13576746	2	37.57833
DUSP22	cg02748245	6	36.96732
PHF21B	cg07828692	22	36.83565
FMOD	cg28491014	1	35.99134
DIP2C	cg03524565	10	35.84642
FABP9	cg05335324	8	34.99268
MGAT4C	cg19099342	12	33.85739
CLVS1	cg18485929	8	33.65325
ULK4	cg01413466	4	32.86652

calculating the significance of its enrichment, a *p*-value will be shown, and a small *p*-value means that differential genes are enriched in this entry. The results, combined with the biological implications, can be used to screen out genes that can be used in subsequent experiments. Figs. 5,6 demonstrate the details. In Fig. 5, it can be observed that genes corresponding to differential methylation sites are enriched in items such as calcium binding, nitrate, and metabolic regulation. In Fig. 6, the genes corresponding to differential methylation sites are enriched in the sensory perception of sound, threonine kinase, protein binding, and other items.

Pathway Analysis

Pathway analysis was used to analyze the genes corresponding to differential methylation sites, and the results showed that small *p*-value also indicated that the genes were enriched in the pathway. In this way, it is possible to see which cell pathways change when a tissue sample differs. Figs. 7,8 illustrate the details. Fig. 7 illustrates that genes corresponding to differential methylation sites are enriched in the transcriptional dysfunction entries in cancer. In Fig. 8, genes corresponding to differential methylation sites are enriched in the bladder cancer entry.

Table 5. The top 10 downregulated sites of differential methylation sites.

Site	Code	Location	Difference value
HLA-C	cg17348343	6	–40.95982
BRSK2	cg01345839	11	–39.53237
RAP1GAP2	cg01847294	17	–38.16347
CPS1	cg12848594	2	–38.03263
HDAC4	cg06839683	2	–37.63653
TMCO3	cg08942815	13	–35.72289
HOXD4	cg14673563	2	–34.84267
PDE1C	cg05948295	7	–33.71169
GRAP2	cg17392658	22	–33.23464
SATB1	cg0428689	3	–32.95347

Cluster Analysis

Fig. 9 shows the cluster analysis results of differentially methylated sites, which helps understand the similarities and differences between samples. The samples were divided into groups by calculating the similarity and distance between the samples. Cluster analysis helps bring samples with similar DNA methylation patterns for further study. If two samples belong to the same group, they are very similar in DNA methylation and have similar biological features. Conversely, if two samples belong to different groups, they may have large differences in DNA methylation. The cluster analysis results can help researchers identify clusters of samples with similar methylation patterns, which may indicate that these samples share certain biological features or associated genetic changes. This is very helpful for understanding the similarities and differences between different samples and studying the relationship between methylation and biological function.

Pyrosequencing Results

As demonstrated in Fig. 10, a total of 7 differentially methylated genes were selected from aortic tissue samples of 8 patients with AD and 8 normal aortic tissue samples and verified by pyrosequencing. The results showed that compared with normal aortic tissue, the methylation up-regulated and down-regulated sites (41.8%, 39.9%, 58.4%, 42.8%, 23.7%, 73.1%, and 21.8%) detected in the aortic tissue of AD patients were consistent with the microarray results. It showed that the experiment is highly feasible.

Discussion

Molecular methods can be used to understand the pathogenesis of the disease in depth and provide a basis for the search for therapeutic targets. In this study, aortic tissue was collected from 8 AD patients and 8 non-AD volunteers. The DNA methylation characteristics in AD patients were studied through whole genome DNA methylation analysis. Based on bioinformatics, the epigenetic characteristics in the course of AD were studied. Finally, pyrosequencing

Journal of
BIOLOGICAL REGULATORS
and Homeostatic Agents

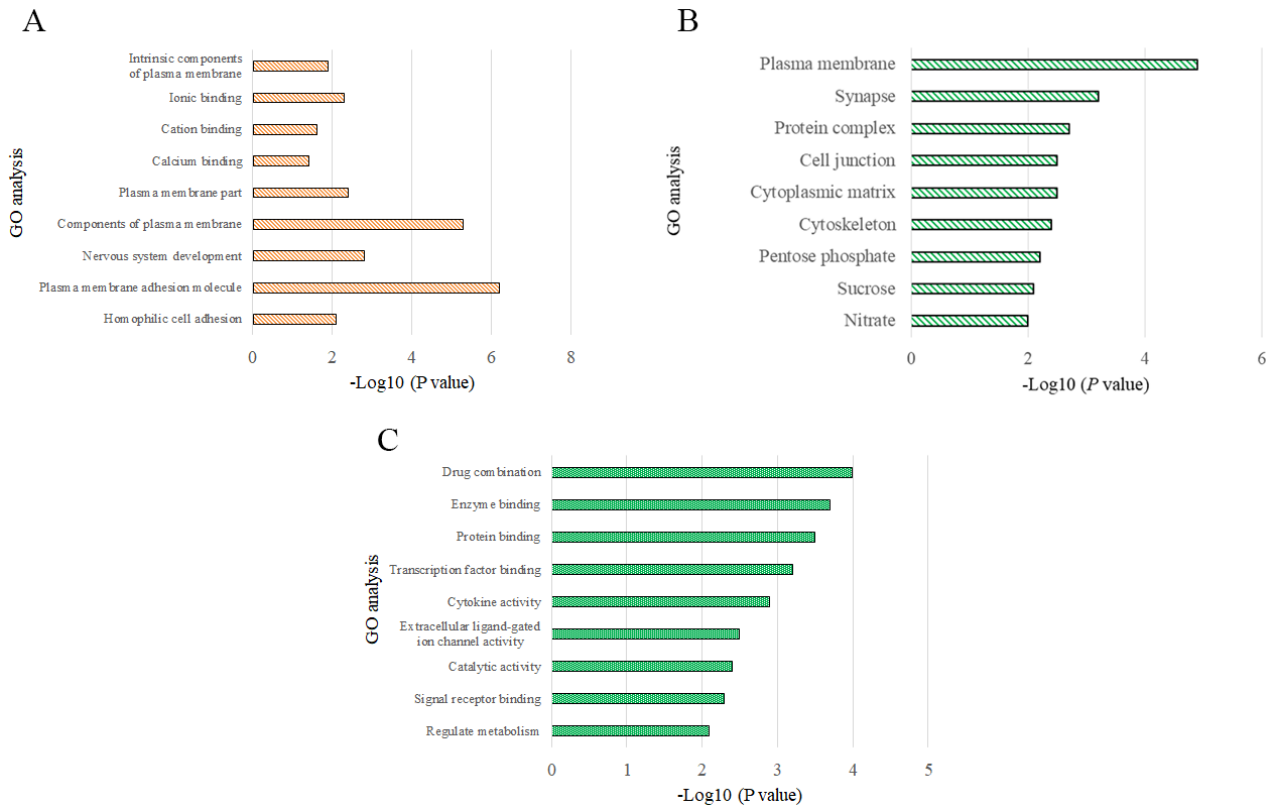

Fig. 5. Gene Ontology (GO) analysis of methylation upregulation in the AD group (partial results). (A) Biological processes, (B) cell components, and (C) molecular functions.

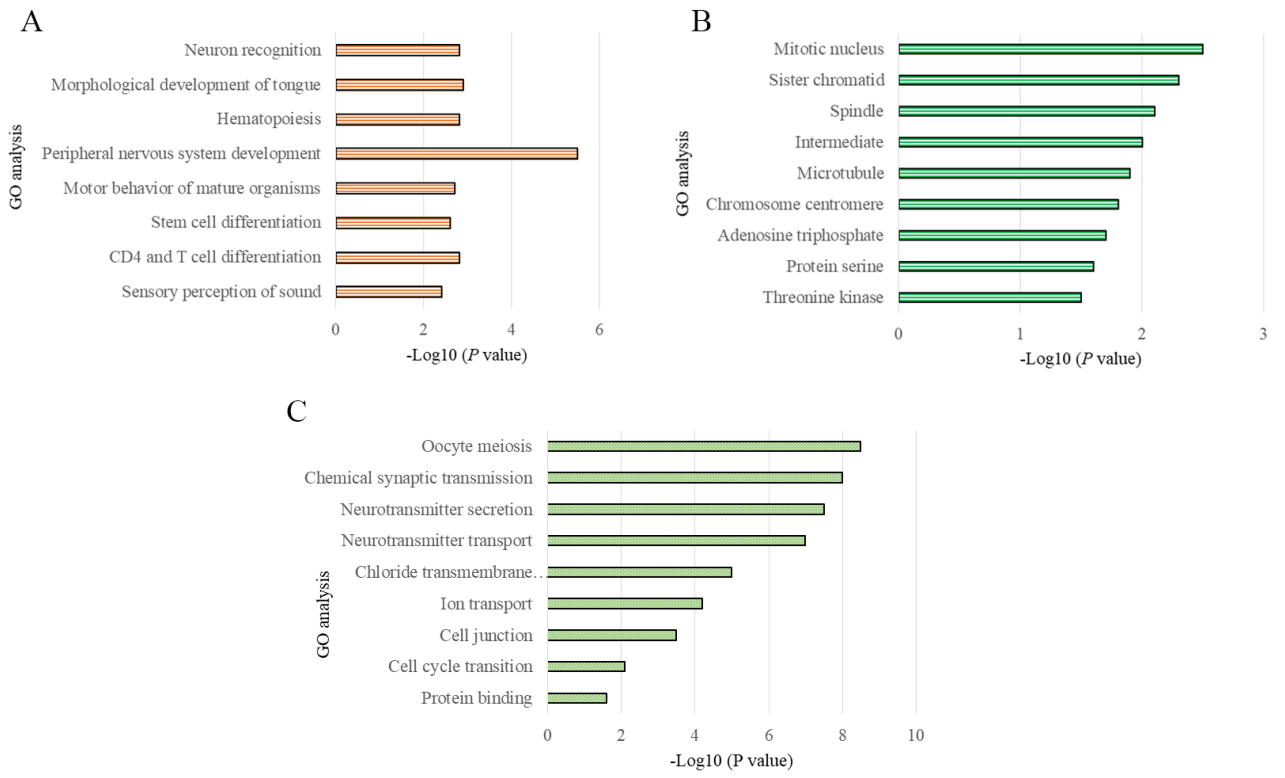

Fig. 6. GO analysis of methylation downregulation in the AD group (partial results). (A) Biological processes, (B) cell components, and (C) molecular functions.

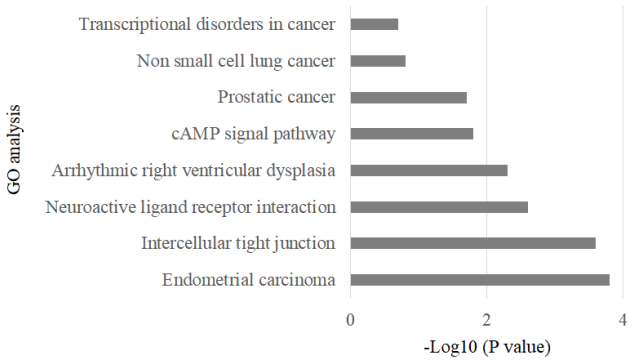

Fig. 7. Pathway analysis of the biological process of methylation upregulation in the AD group (partial results). cAMP, cyclic Adenosine Monophosphate.

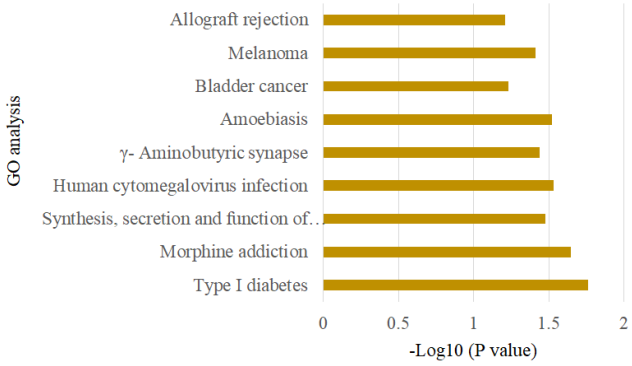

Fig. 8. Pathway analysis of the biological process of methylation downregulation in the AD group (partial results).

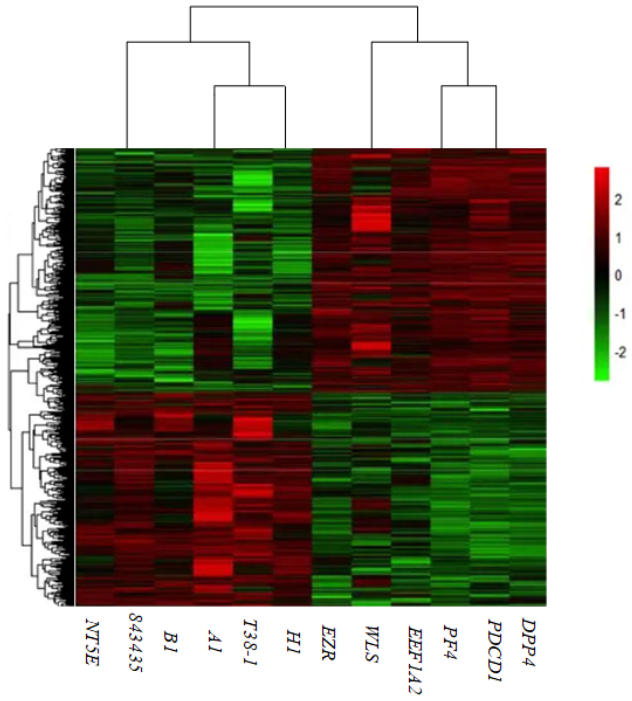

Fig. 9. Cluster analysis results.

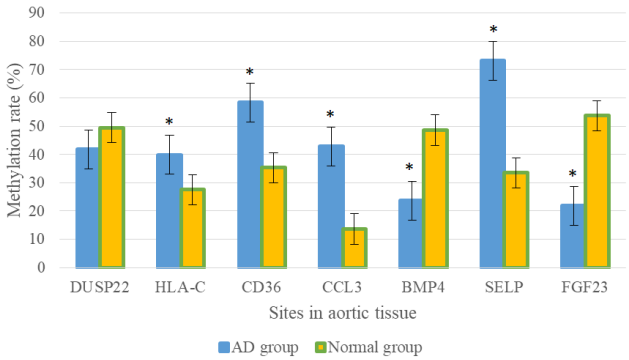

Fig. 10. Pyrosequencing results (partial results). Compared with the normal group, $*p < 0.05$.

was used to verify the accuracy of the chip results. The experiment revealed that there were 1563 sites in total. Compared with the normal group, there were 942 upregulated sites and 621 downregulated sites in the AD group. Considering the quantities of methylation and demethylation contribute to a comprehensive understanding of the dynamic process of DNA methylation, aiding in comprehending the dynamic changes at these sites and identifying sites undergoing demethylation between different groups. The balance between methylation and demethylation is vital for maintaining genomic stability and normal cellular function, facilitating an in-depth exploration of the biological significance of these processes in both normal and diseased states. Also, DNA methylation status might change dynamically during cellular differentiation, development, and disease progression. Simultaneously quantifying methylation and demethylation quantities allows for better capture of these changes, providing more comprehensive information to understand the overall dynamics of methylation within the genome. The differential methylation sites detected by the chip were distributed in Transmission Start Site (TSS) 1500, 5′Untranslated Region (UTR), Genebody, 3′UTR, cytosine, phosphoric acid, Guanine (CpG) island, and off-island CpG sites, mainly in the Genebody. At the same time, GO and pathway analyses were carried out. As mentioned by Kim and Costello (2017) [40], genes whose methylation level was upregulated or downregulated were closely related to cell differentiation, growth, maturity, aging, and death, and they also affected the development of AD to a great extent.

Some studies have suggested [41–43] that DNA methylation may be involved in the pathological mechanism of AD, but the full picture of DNA methylation needs to be explored. Therefore, Chen Y *et al.* (2022) [44] used the Infinium Human methylation 450 K BeadChip to screen DNA methylation patterns in the aortic tissues of 4 patients with Stanford-A AD and 4 controls. The DNA methylation levels of candidate genes were measured by focal sequencing in a replication cohort of 16 AD patients and 7 controls using the Kyoto Encyclopedia of Genes and Genomes

Journal of
BIOLOGICAL REGULATORS
and Homeostatic Agents

(KEGG) pathway and GO analysis. The protein expression levels of candidate genes were evaluated by Western blotting. A total of 589 differentially methylated sites were found in the AD group, including 315 hypomethylated sites and 274 hypermethylated sites. KEGG analysis showed that the differentially methylated location-related genes were enriched in the MAPK signaling pathway, TNF signaling pathway, and apoptosis pathway, and the protein expression level of Fas increased nearly twofold, suggesting that DNA methylation may play a role in the regulation of gene expression. DNA methylation in Stanford-AD aortic tissue is significantly changed, is related to gene dysregulation, and participates in AD progression. This is consistent with the results of this paper. The pathogenesis of AD is still unclear and complicated. In addition to the local rupture or necrosis of elastic fibers in the middle layer of the aorta, mucoid and cyst formation in the matrix, cell inflammation, and changes in protease activity can also be regarded as part of the molecular biology pathogenesis of AD to some extent. The vascular system is considered a very plastic system in which endothelial and smooth muscle cell functions are continuously and dynamically regulated by gene expression under physiological or pathological conditions [45–47].

Methylation is an important regulator of gene expression in epigenetics, and epigenetic research on cardiovascular disease has become a hotspot in recent years. Complex interactions between genes and the environment lead to epigenetic changes in the vasculature, especially endothelial and smooth muscle cells, which play a key role in the pathophysiology of vascular disease. DNA methylation is an important epigenetic DNA modification mechanism that can control many kinds of cells and developmental processes. The epigenetic mechanism of DNA methylation includes the transfer of methyl from S-adenosyl-L-methionine to cytosine of CpG dinucleotide after DNA replication [48–50]. The research results of epigenetics in the medical field have provided solutions to many medical problems. Meanwhile, the correlation between abnormal DNA methylation modification and some serious diseases is being deeply explored, which will provide new ideas for early diagnosis, treatment, and prognosis of diseases. Liu P *et al*. (2021) [51] demonstrated that Thoracic Aortic Dissection (TAD) is a serious disease, and the current understanding of its pathogenesis is limited. While altered DNA methylation is involved in the etiology of many diseases, few studies have examined the role of DNA methylation in the development of TAD. Liu P and other scholars [51] have investigated changes in DNA methylation in TAD and examined ascending aorta tissue from TAD patients and healthy controls by bisulfite whole genome sequencing (WGBS). They found many regions of differential methylation and associated genes enriched in vasculature and cardiac development. These findings suggest that epigenetic regulation is altered in TAD patients. This epigenetic regulation and subsequent alteration in the expression of genes associated with the vascular system and cardiac development, such as Hox family genes, may lead to loss of aortic integrity and TAD pathogenesis.

Proteins encoded by genes control the structure and function of human tissue and organs. DNA methylation can affect the expression of genes, and when the expression of genes changes, it will lead to protein synthesis, thus affecting the structure and function of tissue and organs. The role and importance of abnormal DNA methylation have been confirmed in many diseases, but its role in AD remains unclear. This study used whole genome methylation chip technology to establish the AD whole genome DNA methylation pattern, and the differential methylation sites were screened out based on bioinformatics. Then, GO and pathway analyses were used to analyze and verify the screened differential sites. The results were consistent with the research results of Pan *et al*. (2017) [52]. There are obvious differences between the whole genome DNA methylation of AD patients' aortic tissue and normal aortic tissue, and these gene sites, which are upregulated and downregulated, may play an important role in AD development. This plays an active role in exploring the molecular biological pathogenesis and outcome mechanism of AD and is also helpful in exploring new diagnostic markers and intervention targets for AD in the future.

Conclusion

In this study, DNA methylation characteristics in AD patients were analyzed through whole genome DNA methylation analysis and verification through aortic tissue samples from 8 AD patients and 8 non-AD volunteers. Based on bioinformatics, epigenetic characteristics in the course of AD were studied. Finally, the accuracy of the chip results was verified by pyrosequencing. This study provides a reference for the clinical diagnosis and treatment of AD by exploring the pathogenesis and outcome mechanism from molecular biology. The disadvantage is that the sample size of qualified aortic tissue collected in this study is small, and the experimental results may have certain limitations and one-sidedness. In the future, the sample size will be further expanded to strengthen the findings of this study.

Availability of Data and Materials

All data generated or analyzed in this study are included in this manuscript.

Author Contributions

The design of this study was led by GW, LX, and JN, who made significant contributions to the research philosophy and design. GW and LX conducted experimental research. GW, QJ, JZ and LS provided crucial assistance and advice for experiments. QJ was responsible for data analysis. All authors—QJ, JZ, LS, JN, GW, LX—have con-

tributed to the drafting of research papers or key revisions of important knowledge content. All authors have read and approved the final version to be published. By fully participating in this work, all authors agree to take responsibility for all aspects of the research, ensuring that challenges related to the accuracy or completeness of any part of the paper are appropriately investigated and resolved.

Ethics Approval and Consent to Participate

The study was conducted following the principles outlined in the Declaration of Helsinki. This article has been approved by the Ethics Committee of the Affiliated Hospital of Jiaxing University (Ref. 20210567) and strictly complies with international ethical guidelines. Subject informed consent: All human subjects who participated in the trial signed an informed consent form before participation; the purpose, sampling procedures, potential risks, and benefits of the trial were explained in detail. Privacy and confidentiality: The research team has taken measures to ensure the personal privacy of the subjects and the confidentiality of the data, and all data are processed in anonymous form.

Acknowledgment

Not applicable.

Funding

This research received no external funding.

Conflict of Interest

The authors declare no conflict of interest.

References

[1] Rizza A, Negro F, Mandigers TJ, Palmieri C, Berti S, Trimarchi S. Endovascular Intervention for Aortic Dissection Is "Ascending". International Journal of Environmental Research and Public Health. 2023; 20: 4094.

[2] Sen I, Erben YM, Franco-Mesa C, DeMartino RR. Epidemiology of aortic dissection. Seminars in Vascular Surgery. 2021; 34: 10–17.

[3] Sayed A, Munir M, Bahbah EI. Aortic Dissection: A Review of the Pathophysiology, Management and Prospective Advances. Current Cardiology Reviews. 2021; 17: e230421186875.

[4] Calligaro KD. Optimal treatment of acute uncomplicated type B aortic section: Will a randomized trial ever be conducted? Journal of Vascular Surgery. 2023; 77: 1394.

[5] Okita Y. Aortic dissection is more violent in the young. European Journal of Cardio-Thoracic Surgery. 2023; 63: ezad209.

[6] Liu F, Huang L. Usefulness of ultrasound in the management of aortic dissection. Reviews in Cardiovascular Medicine. 2018; 19: 103–109.

[7] Li T, Liu C, Liu L, Xia H, Xiao Y, Wang X, *et al*. Regulatory Mechanism of MicroRNA-145 in the Pathogenesis of Acute Aortic Dissection. Yonsei Medical Journal. 2019; 60: 352–359.

[8] Bashir M, Tan SZ, Jubouri M, Coselli J, Chen EP, Mohammed I, *et al*. Uncomplicated Type B Aortic Dissection: Challenges in Diagnosis and Categorization. Annals of Vascular Surgery. 2023; 94: 92–101.

[9] Bhardwaj H, Tomar P, Sakalle A, Ibrahim W. EEG-Based Personality Prediction Using Fast Fourier Transform and DeepLSTM Model. Computational Intelligence and Neuroscience. 2021; 2021: 6524858.

[10] Qiu JT, Zhang L, Luo XJ, Yang J, Liu S, Jiang WX, *et al*. Correlation between of aortic dissection onset and climate change. Chinese Journal of Surgery. 2018; 56: 74–77. (In Chinese)

[11] Cheng M, Yang Y, Xin H, Li M, Zong T, He X, *et al*. Noncoding RNAs in aortic dissection: From biomarkers to therapeutic targets. Journal of Cellular and Molecular Medicine. 2020; 24: 11622–11637.

[12] Ou L, Liu HR, Shi XY, Peng C, Zou YJ, Jia JW, *et al*. Terminalia chebula Retz. aqueous extract inhibits the Helicobacter pylori-induced inflammatory response by regulating the inflammasome signaling and ER-stress pathway. Journal of Ethnopharmacology. 2024; 320: 117428.

[13] Yin ZQ, Han H, Yan X, Zheng QJ. Research Progress on the Pathogenesis of Aortic Dissection. Current Problems in Cardiology. 2023; 48: 101249.

[14] Meng X, Han J, Wang L, Wu Q. Aortic dissection during pregnancy and postpartum. Journal of Cardiac Surgery. 2021; 36: 2510–2517.

[15] Liu H, Tang T. A bioinformatic study of IGFBPs in glioma regarding their diagnostic, prognostic, and therapeutic prediction value. American Journal of Translational Research. 2023; 15: 2140–2155.

[16] Zhou Y, Wang T, Fan H, Liu S, Teng X, Shao L, *et al*. Research Progress on the Pathogenesis of Aortic Aneurysm and Dissection in Metabolism. Current Problems in Cardiology. 2024; 49: 102040.

[17] Coppedè F. Mitochondrial DNA methylation and mitochondria-related epigenetics in neurodegeneration. Neural Regeneration Research. 2024; 19: 405–406.

[18] Kumar S, Shanker OR, Banerjee J, Tripathi M, Chandra PS, Dixit AB. Epigenetics in epilepsy. Progress in Molecular Biology and Translational Science. 2023; 198: 249–269.

[19] Koletzko B. Epigenetics, Nutrition and Growth. World Review of Nutrition and Dietetics. 2023; 126: 70–85.

[20] Kumar A, Sinha N, Bhardwaj A, Goel S. Clinical risk assessment of chronic kidney disease patients using genetic programming. Computer Methods in Biomechanics and Biomedical Engineering. 2022; 25: 887–895.

[21] Zhou S, Wang X, Gao H, Zeng Y. DNA Methylation in Pulmonary Fibrosis. Advances in Experimental Medicine and Biology. 2020; 1255: 51–62.

[22] Karakaidos P, Karagiannis D, Rampias T. Resolving DNA Damage: Epigenetic Regulation of DNA Repair. Molecules. 2020; 25: 2496.

[23] Fernandez A, O'Leary C, O'Byrne KJ, Burgess J, Richard DJ, Suraweera A. Epigenetic Mechanisms in DNA Double Strand Break Repair: A Clinical Review. Frontiers in Molecular Biosciences. 2021; 8: 685440.

[24] Kuznetsov NA, Kanazhevskaya LY, Fedorova OS. DNA Demethylation in the Processes of Repair and Epigenetic Regulation Performed by 2-Ketoglutarate-Dependent DNA Dioxygenases. International Journal of Molecular Sciences. 2021; 22: 10540.

[25] Garner IM, Brown R. Is There a Role for Epigenetic Therapies in Modulating DNA Damage Repair Pathways to Enhance Chemotherapy and Overcome Drug Resistance? Cancers. 2022; 14: 1533.

[26] Prasher D, Greenway SC, Singh RB. The impact of epigenetics on cardiovascular disease. Biochemistry and Cell Biology = Biochimie et Biologie Cellulaire. 2020; 98: 12–22.

[27] Cao J, Wu Q, Huang Y, Wang L, Su Z, Ye H. The role of DNA methylation in syndromic and non-syndromic congenital heart disease. Clinical Epigenetics. 2021; 13: 93.

[28] Palou-Márquez G, Subirana I, Nonell L, Fernández-Sanlés A, Elosua R. DNA methylation and gene expression integration in cardiovascular disease. Clinical Epigenetics. 2021; 13: 75.

[29] Xia Y, Brewer A, Bell JT. DNA methylation signatures of incident coronary heart disease: findings from epigenome-wide association studies. Clinical Epigenetics. 2021; 13: 186.

[30] Chen X, Yan F, Lin X, Shi L, Wang X, Zeng Y. DNA Methylation in Chronic Obstructive Pulmonary Disease. Advances in Experimental Medicine and Biology. 2020; 1255: 83–98.

[31] van Breugel M, Qi C, Xu Z, Pedersen CET, Petoukhov I, Vonk JM, *et al*. Nasal DNA methylation at three CpG sites predicts childhood allergic disease. Nature Communications. 2022; 13: 7415.

[32] Tabaei S, Tabaee SS. DNA methylation abnormalities in atherosclerosis. Artificial Cells, Nanomedicine, and Biotechnology. 2019; 47: 2031–2041.

[33] Krolevets M, Cate VT, Prochaska JH, Schulz A, Rapp S, Tenzer S, *et al*. DNA methylation and cardiovascular disease in humans: a systematic review and database of known CpG methylation sites. Clinical Epigenetics. 2023; 15: 56.

[34] Cuadrat RRC, Kratzer A, Arnal HG, Rathgeber AC, Wreczycka K, Blume A, *et al*. Cardiovascular disease biomarkers derived from circulating cell-free DNA methylation. NAR Genomics and Bioinformatics. 2023; 5: lqad061.

[35] Miller K, Webster J, Imus P, Ament C, Hardy M, Zou YS. Detection of an atypical BCR::ABL1 fusion in a patient with secondary B-cell acute lymphoblastic leukemia/lymphoma following multiple myeloma treatment. Cancer Genetics. 2023; 274-275: 30–32.

[36] Li Y, Liu H. Clinical powers of Aminoacyl tRNA Synthetase Complex Interacting Multifunctional Protein 1 (AIMP1) for head-neck squamous cell carcinoma. Cancer Biomarkers: Section a of Disease Markers. 2022; 34: 359–374.

[37] Ou L, Zhu Z, Hao Y, Li Q, Liu H, Chen Q, *et al*. 1,3,6-Trigalloylglucose: A Novel Potent Anti-*Helicobacter pylori* Adhesion Agent Derived from Aqueous Extracts of *Terminalia chebula* Retz. Molecules. 2024; 29: 1161.

[38] Yang T, Liu X, Kumar SK, Jin F, Dai Y. Decoding DNA methylation in epigenetics of multiple myeloma. Blood Reviews. 2022; 51: 100872.

[39] Wongchai A, Jenjeti R. Priyadarsini I, Deb N, Bhardwaj A, Tomar P. Farm monitoring and disease prediction by classification based on deep learning architectures in sustainable agriculture. Ecological Modelling. 2022; 474: 110167.

[40] Kim M, Costello J. DNA methylation: an epigenetic mark of cellular memory. Experimental & Molecular Medicine. 2017; 49: e322.

[41] Anil VT, Nawaf A, Abdulrhman MA, Olfat MM, Arpit B, Bharat S. Multispectralimage analysis for monitoring by IoT based wireless communication using secure locations protocol and classification by deep learning techniques. Optik. 2022; 271: 170122.

[42] Skorvanova M, Matakova T, Skerenova M, Sarlinova M, Drobkova H, Petras M, *et al*. Methylation of MMP2, TIMP2, MMP9 and TIMP1 in abdominal aortic aneurysm. Bratislavske Lekarske Listy. 2020; 121: 717–721.

[43] Halawa S, Latif N, Tseng YT, Ibrahim AM, Chester AH, Moustafa A, *et al*. Profiling Genome-Wide DNA Methylation Patterns in Human Aortic and Mitral Valves. Frontiers in Cardiovascular Medicine. 2022; 9: 840647.

[44] Chen Y, Xu X, Chen Z, Huang B, Wang X, Fan X. DNA methylation alternation in Stanford- A acute aortic dissection. BMC Cardiovascular Disorders. 2022; 22: 455.

[45] Verstraeten A, Fedoryshchenko I, Loeys B. The emerging role of endothelial cells in the pathogenesis of thoracic aortic aneurysm and dissection. European Heart Journal. 2023; 44: 1262–1264.

[46] Chen Y, Zhang T, Yao F, Gao X, Li D, Fu S, *et al*. Dysregulation of interaction between LOX^{high} fibroblast and smooth muscle cells contributes to the pathogenesis of aortic dissection. Theranostics. 2022; 12: 910–928.

[47] Xu H, Zhang B, Li Y, Yang F, Liu Y, Xu Z, *et al*. Dysregulated long non-coding RNAs involved in regulation of matrix degradation during type-B aortic dissection pathogenesis. General Thoracic and Cardiovascular Surgery. 2021; 69: 238–245.

[48] Nakamura R, Honda K, Yuzaki M, Nishimura Y. Severe aortic regurgitation with intimal intussusception secondary to Debakey type I aortic dissection. Echocardiography. 2020; 37: 652–653.

[49] Mancia A. Genome-Wide DNA Methylation Protocol for Epigenetics Studies. Methods in Molecular Biology. 2022; 2498: 19–41.

[50] Jiaqing H, Linlin W. Abu Bakkar S, Zulkiflee A, Arpit B. Bharat S. Forecasting GHG emissions for environmental protection with energy consumption reduction from renewable sources: A sustainable environmental system. Ecological Modelling. 2023; 475: 110181.

[51] Liu P, Zhang J, Du D, Zhang D, Jin Z, Qiu W, *et al*. Altered DNA methylation pattern reveals epigenetic regulation of Hox genes in thoracic aortic dissection and serves as a biomarker in disease diagnosis. Clinical Epigenetics. 2021; 13: 124.

[52] Pan S, Lai H, Shen Y, Breeze C, Beck S, Hong T, *et al*. DNA methylome analysis reveals distinct epigenetic patterns of ascending aortic dissection and bicuspid aortic valve. Cardiovascular Research. 2017; 113: 692–704.